Evaluation of the MODIS Albedo product over a heterogeneous agricultural area

J.A. Sobrino [a] , B. Franch [a] , R. Oltra-Carrió [a] , E.F. Vermote [b] & E.
Fedele [b]

[a] Global Change Unit, Image Processing Laboratory (UCG-IPL) ,
Parque Cientifico, Universitat de Valencia , Valencia , Spain
[b] Department of Geographical Sciences , University of Maryland ,
College Park , MD , USA
Published online: 30 Apr 2013.

PLEASE SCROLL DOWN FOR ARTICLE

Taylor & Francis
Taylor & Francis Group

Evaluation of the MODIS Albedo product over a heterogeneous agricultural area

J.A. Sobrino[a]*, B. Franch[a], R. Oltra-Carrió[a], E.F. Vermote[b], and E. Fedele[b]

[a]Global Change Unit, Image Processing Laboratory (UCG-IPL), Parque Científico, Universitat de Valencia, Valencia, Spain; [b]Department of Geographical Sciences, University of Maryland, College Park, MD, USA

In this article, the Moderate Resolution Imaging Spectroradiometer (MODIS) Bidirectional Reflectance Distribution Function (BRDF)/Albedo product (MCD43) is evaluated over a heterogeneous agricultural area in the framework of the Earth Observation: Optical Data Calibration and Information Extraction (EODIX) project campaign, which was developed in Barrax (Spain) in June 2011. In this method, two models, the RossThick-LiSparse-Reciprocal (RTLSR) (which corresponds to the MODIS BRDF algorithm) and the RossThick-Maignan-LiSparse-Reciprocal (RTLSR-HS), were tested over airborne data by processing high-resolution images acquired with the Airborne Hyperspectral Scanner (AHS) sensor. During the campaign, airborne images were retrieved with different view zenith angles along the principal and orthogonal planes. Comparing the results of applying the models to the airborne data with ground measurements, we obtained a root mean square error (RMSE) of 0.018 with both RTLSR and RTLSR-HS models. The evaluation of the MODIS BRDF/Albedo product (MCD43) was performed by comparing satellite images with AHS estimations. The results reported an RMSE of 0.04 with both models. Additionally, taking advantage of a homogeneous barley pixel, we compared *in situ* albedo data to satellite albedo data. In this case, the MODIS albedo estimation was (0.210 ± 0.003), while the *in situ* measurement was (0.204 ± 0.003). This result shows good agreement in regard to a homogeneous pixel.

Introduction

Land surface broadband albedo is a critical land physical parameter affecting the Earth's climate. It is well recognized that surface albedo is among the main radiative uncertainties in current climate modelling. In fact, an absolute accuracy of 0.02–0.05 is required for albedo characterization at spatial and temporal scales compatible with climate studies (Sellers 1993). The increasing spatial resolution of modern climate models makes it necessary to examine the spatial features of global surface albedo. Satellite remote sensing provides the only practical way of producing high-quality global albedo data sets with high spatial and temporal resolution.

The Moderate Resolution Imaging Spectroradiometer (MODIS) on board the Terra and Aqua satellites provides near-global earth observations on a daily basis, with fine spectral and spatial resolution (Barnes, Pagano, and Salomonson 1998). The availability of

*Corresponding author. Email: sobrino@uv.es

MODIS products is supposed a great advance as these products are widely used by the scientific community with different purposes as, for example, the evaluation of deforestation (Ferreira et al. 2007), estimation of evapotranspiration (Mu et al. 2007), and studies on snow cover (Pu, Xu, and Salomonson 2007). The MODIS Bidirectional Reflectance Distribution Function (BRDF)/Albedo product, MCD43 (Strahler et al. 1999), combines registered, multidate, multiband, atmospherically corrected surface reflectance data from the MODIS and Multi-angle Imaging Spectroradiometer (MISR) instruments to fit a BRDF in seven spectral bands at 1 km spatial resolution on a 16 day cycle. From this characterization of the surface anisotropy, the algorithm performs angular integrations to derive intrinsic land surface albedos for each spectral band and three broadbands covering the solar spectrum. However, in this article, we work directly with the MCD43A1 product, which contains three-dimensional (3D) data sets providing users with weighting parameters for the models used to derive the Albedo and BRDF products. Both Terra and Aqua data are used in the generation of this product, providing the highest probability for quality input data and designating it as an MCD, meaning combined product.

The validation of this product has been studied in previous works. Jin et al. (2003) evaluated the accuracy of the MODIS albedo product using only observations from the MODIS instrument aboard the Terra platform and over homogeneous regions at local solar noon. They found that the MODIS albedo product met an absolute accuracy requirement of 0.02 in spring and summer, identifying these as the growing seasons. However, during the winter season, they observed lower albedo estimations than the field values. Liang et al. (2002) validated the MODIS black-sky albedo product, scaling up the ground measurements to MODIS resolution using high-resolution Enhanced Thematic Mapper Plus (ETM+) imagery. In this work, the authors considered that the surface is Lambertian, so the retrieved surface reflectance of different spectral bands is equivalent to surface spectral albedos. Despite this approach, the comparison showed good agreement. Roesch, Schaaf, and Gao (2004) compared MODIS albedo at 0.05° with *in situ* measurements collected at Baseline Surface Radiation Network sites during snow-free periods. The results showed good agreement, although MODIS generally underestimated reflectivity. Coddington et al. (2008) compared the spectral surface albedo derived from the airborne Solar Spectral Flux Radiometer (SSFR) with the MODIS albedo product. They centred the analysis over two sites (an urban area and a ranchland whose primary vegetation cover was parched grass); where *in situ* albedo measurements were retrieved during the campaign. Their results showed a MODIS underestimation of 0.025–0.05 at the urban area and a MODIS overestimation of 0.02–0.05 at the rural area regarding the SSFR results. Liu et al. (2009) evaluated the ability of the MODIS albedo product to represent albedos at all diurnal solar zenith angles through a comparison with field measurements from the Surface Radiation Budget Network (SURFRAD) and Atmospheric Radiation Measurement Southern Great Plains (ARM/SGP). They found a high correlation between *in situ* and satellite albedos for almost all cases. They observed negative mean biases, with magnitude increased as solar zenith angle increased, meaning that the MODIS algorithm underestimates albedo as compared with ground measurements. Cescatti et al. (2012) recently compared MODIS albedo retrievals with surface measurements taken at 53 FLUXNET sites that met strict conditions of land cover homogeneity. They observed good agreement for forest sites. In contrast, in the case of non-forest sites with larger albedo values (grasslands and croplands), MODIS generally underestimated *in situ* measurements across the seasonal cycle.

The goal of this work is to evaluate the MODIS albedo product over a heterogeneous agricultural area using *in situ* albedo measurements in addition to airborne hyperspectral imagery. We will analyse two different BRDF models, i.e. on the one hand, the same model

as the MODIS product and, on the other, the improvement in this model as proposed by Maignan, Breon, and Lacaze (2004) that corrects the hot spot effect. The whole dataset presented in this work was acquired during the EODIX field campaign.

Material and methodology

Study area and field campaign

Barrax is located in southeastern Spain, within La Mancha, a plateau 700 m above sea level, and it is in the western part of the province of Albacete, 28 km from the city of Albacete (39° 3′ N, 2° 60′ W). The area is characterized by a flat morphology (elevation range up to 2 m only) and large, uniform land-use units. The dominant cultivation pattern in the 10,000 ha area is approximately 65% dry land (two-thirds winter cereals, one-third fallow) and 35% irrigated crops (75% corn, 15% barley, and 10% others, including alfalfa) (Moreno et al. 2001). The climate of Barrax is of the Mediterranean type, with heavy rainfall in spring and autumn and dry in summer. It presents a high level of continentality, with quite sudden changes from cold to warm months and high oscillation in all seasons between maximum and minimum daily temperatures.

Several remote-sensing field campaigns have been carried out over the Barrax test site during recent years, such as the SPARC 2004 field campaign (Sobrino et al. 2009), which established Barrax as an appropriate site for the calibration/validation process using remote-sensing images. This article is focused on the field campaign developed within the framework of the EODIX project. It was carried out from the 10th to the 12th of June 2011, where extensive *in situ* and airborne measurements were carried out over several crops and natural areas.

In situ *data*

Calibration and validation activities were carried out simultaneously to the airborne overpass. In this article, we distinguish two types of *in situ* measurements: surface reflectance and albedo measurements. On the one hand, surface reflectance was retrieved over different surface types of the test area in order to obtain sufficient representative spectra. A transect concurrent with the airborne overpass, starting 30 min before and ending 30 min after, was performed with a FieldSpec 3 spectroradiometer (Analytical Spectral Devices, Inc., Boulder, CO, USA). In this way, four different fields were characterized: bare soil, alfalfa, barley, and green grass. Additionally, a goniometer was placed in a corn field with a GER 1500 spectroradiometer (Spectra Vista Corporation, Poughskeepsie, NY, USA) (Figure 1(*a*)). The nadir measurements retrieved during the airborne overpass were also considered in the validation. On the other hand, we disposed of albedo measurements from two albedometers located at two meteorological stations, one in a barley field (Figure 1(*b*)) and the other in a wheat field (Figure 1(*c*)). Furthermore, angular surface reflectance measurements from the goniometer were inverted in order to estimate surface albedo.

Finally, the aerosol optical thickness (AOT) needed in atmospheric correction was retrieved with a CE318 sun-photometer (Cimel Electronique S.A.S., Paris, France). The CE318 is a commercial sun-photometer designed for the automatic measurement of direct solar irradiance and sky radiance. The unit employed in this campaign was an extended version, measuring in channels centred at 340, 380, 440, 500, 670, 870, 940, 1020, and 1640 nm, with the 940 nm channel being dedicated to obtaining atmospheric columnar water vapour.
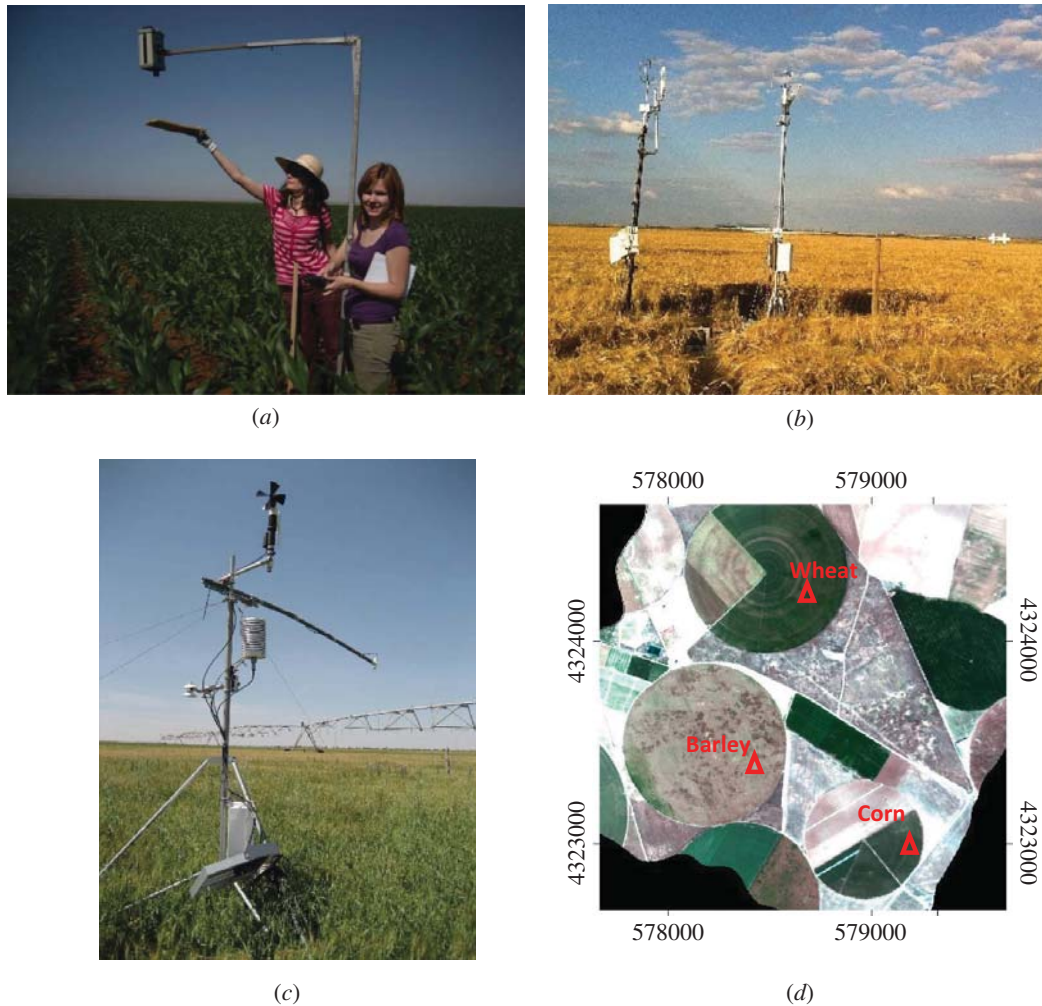
Figure 1. *In situ* albedo measurements from (*a*) a goniometer in a corn field, (*b*) an albedometer located in a barley field at a meteorological station in a barley field, and (*c*) an albedometer located in a wheat field at a meteorological station. (*d*) AHS RGB (*red–green–blue*) image (coordinates in UTM) and positions of the validation points (*triangles*).

Airborne data

The airborne data studied in this work were acquired by the Airborne Hyperspectral Scanner (AHS) (Sobrino et al. 2009), which is an 80 band airborne imaging radiometer, developed and built by SensyTech Inc. (Beverly, MA, USA) (currently Argon ST, formerly DaedalusEnt. Inc.) and operated by the Spanish Institute for Aerospace Technology (INTA). It has 63 bands in the reflective part of the electromagnetic spectrum, seven in the 3–5 μm range and 10 in the 8–13 μm region. However, our study will be centred on the bands equivalent to MODIS. Table 1 shows the equivalence that was considered between the sensors.

The AHS is a line scanner based on a concept shared with classical airborne line scanners, such as the Airborne Thematic Mapper (ATM), Multispectral Infrared and Visible Imaging Spectrometer (MIVIS), and MODIS Airborne Simulator (MAS). The AHS was installed in a CASA-212 200 Series aircraft, and integrated with a GPS unit from Applanix (Richmond Hill, ON, Canada).

Table 1.   Equivalence between AHS and MODIS bands.

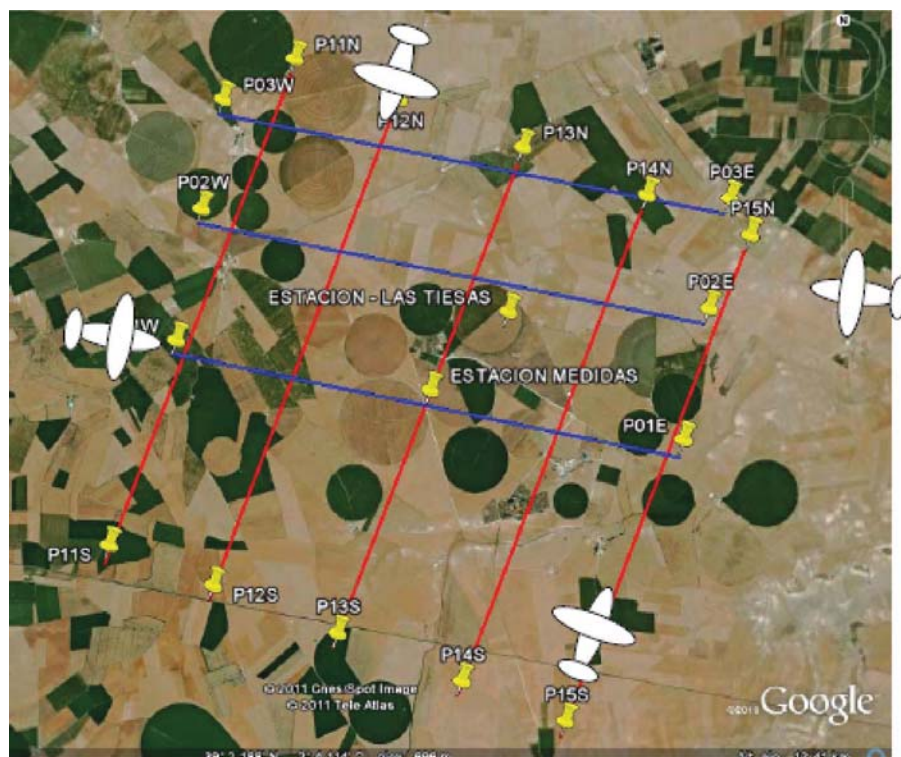| MODIS	AHS
Band 1: (645 ± 25) nm	Band 8: (650 ± 14) nm
Band 2: (859 ± 18) nm	Band 15: (856 ± 14) nm
Band 3: (469 ± 10) nm	Band 2: (471 ± 14) nm
Band 4: (555 ± 10) nm	Band 5: (560 ± 14) nm
Band 5: (1240 ± 10) nm	Band 20: (1001 ± 14) nm
Band 6: (1640 ± 12) nm	Band 21: (1588 ± 45) nm
Band 7: (2130 ± 25) nm	Band 35: (2134 ± 45) nm

Figure 2.   Flight lines along the principal plane (blue) and the orthogonal plane (red) over the test area, 12 June 2011.

The data used in this work were acquired in a straight line at an altitude of 2545 m above sea level on the 12th of June 2011. The resulting data have a ground spatial resolution of 4 m. During this campaign, several flights were achieved from 09.00 to 10.00 UTC in order to obtain enough bidirectional observations to retrieve the BRDF of the test area. Figure 2 shows the flight lines carried out. These were planned considering the symmetry of BRDF in the orthogonal plane. In order to detect view zenith angles near to 60° during flights, a wedge was placed under the AHS, tilting the sensor developed along the furthest flight lines in regard to the main area.

Methodology

The MCD43A1 MODIS product is estimated using a kernel-based BRDF model (Strahler et al. 1999). The theoretical basis of this semi-empirical model is that land surface reflectance, ρ, is modelled as a sum of three kernels (k_0, k_1, and k_2) (Equation (1)) representing basic scattering types: isotropic scattering, radiative transfer-type volumetric

scattering (as from horizontally homogeneous leaf canopies), and geometric-optical surface scattering (as from scenes containing three-dimensional objects that cast shadows and are mutually obscured from view at off-nadir angles):

$$\rho\,(\theta_s, \theta_v, \phi) = k_0 + k_1\,F_1\,(\theta_s, \theta_v, \phi) + k_2\,F_2(\theta_s, \theta_v, \phi), \tag{1}$$

where θ_s is the sun zenith angle, θ_v is the view zenith angle, ϕ is the relative azimuth angle, F_1 is the volume-scattering kernel (based on the Rossthick function derived by Roujean, Leroy, and Deschamps (1992)), and F_2 is the geometric kernel (based on the LiSparse-Reciprocal model (Li and Strahler 1992), but considering the reciprocal form given by Lucht (1998)), F_1 and F_2 are fixed functions of the observation geometry, but k_0, k_1, and k_2 are free parameters. The MCD43 product, which combines Terra and Aqua data, is estimated by inverting the BRDF model parameters over a composite period of 16 days in which the surface is assumed to be stable. In this article, we evaluate the RossThick-LiSparse-Reciprocal (RTLSR) BRDF model, which is the model considered in the MCD43 MODIS product, and the same model but corrected for the hot spot process, as proposed by Maignan, Breon, and Lacaze (2004) (RTLSR-HS).

The albedo is derived by integrals of the BRDF model through the black-sky albedo (α_{bs}) and the white-sky albedo (α_{ws}):

$$\alpha_{bs}\,(\theta, \Lambda) = \sum_k f_k\,(\Lambda)\,h_k\,(\theta), \tag{2}$$

$$\alpha_{ws}\,(\Lambda) = \sum_k f_k\,(\Lambda)\,H_k, \tag{3}$$

where θ is the solar zenith angle, Λ is the wavelength, f_k is the BRDF kernel model,

$$h_k\,(\theta) = \int_0^{2\pi} \int_0^{\pi/2} K_k(\theta, \vartheta, \phi)\sin\vartheta\,\cos\vartheta\,\mathrm{d}\vartheta, \text{ and} \tag{4}$$

$$H_k = 2\int_0^{\pi/2} h_k\,(\theta)\sin\theta\,\cos\theta\,\mathrm{d}\theta, \tag{5}$$

where K_k are the kernel parameters, ϑ is the view zenith angle, and φ is the relative azimuth. By interpolating between black-sky and white-sky albedo quantities, the following equation can be used to compute MODIS blue-sky (or actual or instantaneous) albedo, α:

$$\alpha\,(\theta, \Lambda) = [1 - S\,(\theta, \tau\,(\Lambda))]\,\alpha_{bs}\,(\theta, \Lambda) + S\,(\theta, \tau\,(\Lambda))\,\alpha_{ws}\,(\Lambda), \tag{6}$$

where S is the fraction of diffuse skylight that depends on aerosol optical depth τ and on wavelength Λ. This parameter was derived from 6S for each airborne image.

Finally, the spectral to broadband conversion was achieved following Liang (2001), which in the particular case of MODIS is written as

$$\alpha_{broadband} = 0.160\alpha_1 + 0.291\alpha_2 + 0.243\alpha_3 + 0.116\alpha_4 + 0.112\alpha_5 + 0.081\alpha_7 - 0.0015,$$

where α_i is the blue-sky albedo for band i.

In this article, we first corrected atmospherically the airborne images with the radiative transfer code 6S (Vermote et al. 2006) before deriving BRDF. Next, we obtained the white-sky albedo, the black-sky albedo and, with the fraction of diffuse skylight, the

blue-sky albedo. Next, we estimated the blue-sky broadband albedo, which was evaluated with *in situ* measurements. In addition, since the MCD43A1 MODIS product consists of the BRDF parameters, we derived the blue-sky broadband albedo following the same methodology as for airborne data and considering the same angular conditions. Finally, we compared airborne images with MODIS blue-sky broadband albedo images.

Results

Atmospheric correction

First, airborne images were atmospherically corrected with 6S. We corrected only AHS bands equivalent to MODIS bands (Table 1). Surface reflectance images were tested with *in situ* measurements. A total of five different surfaces were taken into account: corn, bare soil, alfalfa, barley, and green grass. Since each surface was observed by AHS at different angles and *in situ* measurements were retrieved at nadir, we considered only airborne images that observed each validation point with view zenith angles lower than 25°. Figure 3 shows airborne versus *in situ* surface reflectance, taking into account every flight (for this condition) and every surface. In this graph, singular *in situ* values present different airborne estimations and, beyond these, the points most dispersed correspond to higher view zenith angles. Table 2 shows the bias, standard deviation, and RMSE.

Airborne albedo estimation

Once tested, we obtained the BRDF from the surface reflectivity airborne images. First, we georeferenced every image and extracted the common area for every image. Then, we inverted the models by using a least-squares method, followed by estimation of white- and black-sky albedo following Equations (2) and (3). Since black-sky albedo depends upon the solar zenith angle, each airborne image had a different black-sky albedo but the same white-sky albedo. Finally, with the fraction of diffuse skylight, we derived the blue-sky albedo following Equation (4) and transferred from narrow to broadband albedo following Liang (2001). Figure 1(*d*) shows the position of the three validation points considered: two meteorological stations (one in a barley field and the other in a wheat field) and a
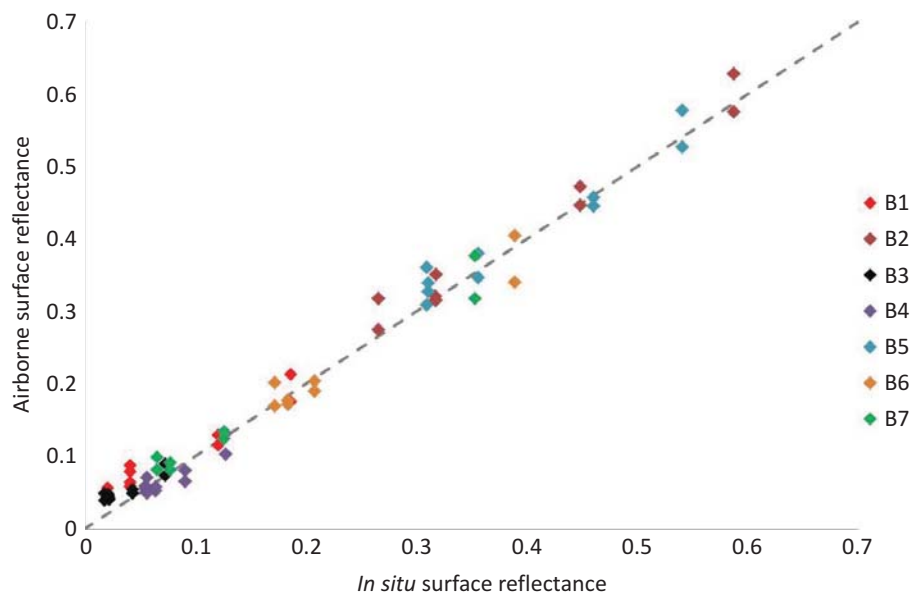

Figure 3. Airborne surface reflectance testing of *in situ* measurements for bands 1 to 7 (B1–B7).

Table 2. Statistics when testing surface reflectance airborne images with *in situ* data.

	Bias	Standard deviation	RMSE
Band 8 (MODIS Band 1)	0.020	0.019	0.030
Band 15 (MODIS Band 2)	0.015	0.020	0.030
Band 2 (MODIS Band 3)	0.017	0.009	0.020
Band 5 (MODIS Band 4)	−0.006	0.013	0.014
Band 20 (MODIS Band 5)	0.012	0.020	0.030
Band 21 (MODIS Band 6)	−0.004	0.020	0.020
Band 35 (MODIS Band 7)	0.007	0.019	0.020

goniometer in a corn field. Figure 4 shows the airborne versus *in situ* blue-sky albedo broadband estimation. Since we disposed of eight different flights that were performed over 1 hour (09.00–10.00 UTC), we averaged the albedo obtaining three different measurements representing the albedo corresponding to the times 09.00, 9:30, and 10.00. We must emphasise that the albedo of the corn field, which was derived from the goniometer, corresponds to the visible blue-sky albedo, since the GER radiometer (used in the goniometer) does not cover wavelenghts greater than 1500 nm. Thus, it was compared with the airborne visible blue-sky albedo. Additionally, the *in situ* corn albedo was estimated with both models. From the plot, we observed that both models yielded similar results, with high correlation coefficients showing good agreement between airborne and *in situ* albedo values. The worst correlation was found for the barley field, where both models underestimated the *in situ* measurement. The greatest difference between the models was for the corn field. While the RTLSR-HS model provided good estimation, the RTLSR model underestimated it slightly. Finally, both RTLSR and the RTLSR-HS models yielded an RMSE of 0.018.

Aggregation

After testing AHS albedo images, we aggregated them into the MODIS spatial resolution (500 m). We assumed a linear average of the high-resolution AHS image in order to
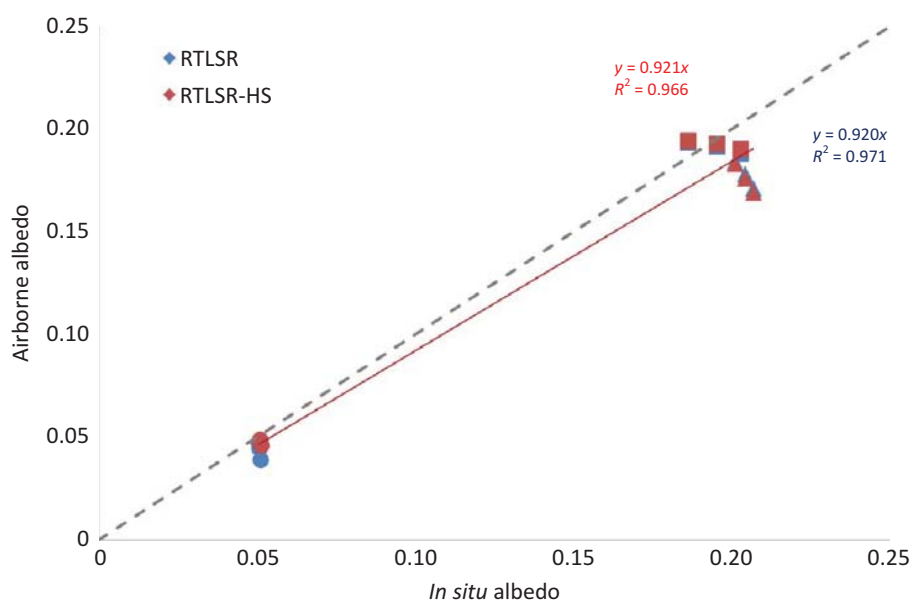

Figure 4. Results of the albedo test carried out in the corn (*circles*), wheat (*squares*), and barley (*triangles*) fields.

compare both products directly. Figure 5 shows an example of the difference between AHS and MODIS resolutions and the location of the MODIS nearest pixels to *in situ* albedo measurements. The equivalence between the MODIS pixels over the AHS image shows that in the case of the barley field, the MODIS pixel was homogeneous, while in the case of the wheat and corn fields, they were heterogeneous. Figure 6 represents the albedo derived from the MODIS product versus that estimated from AHS images for these pixels. First, we observed that the MODIS albedo did not change significantly between each surface. In the case of the AHS albedo derived from the RTLSR BRDF model, the difference between each pixel is lower than that in the RTLSR-HS model. Second, the MODIS albedo estimations were higher than AHS albedos. The greatest difference between the albedo estimated from the RTLSR-HS model and the MODIS product was found in the corn field pixel, which was the most heterogeneous (as shown by the error bars in the plot). The RMSE obtained by comparing AHS to the MODIS albedo product was 0.04 for both models. Third, in regard to the barley field, whose MODIS pixel was homogeneous, the *in situ* and satellite albedos were comparable (MODIS and *in situ* albedo measurements were 0.210 ± 0.003 and 0.204 ± 0.003, respectively. This individual case shows that the MODIS product presents good agreement with *in situ* data in regard to a homogeneous pixel.

Discussion and conclusion

The aim of this study was to evaluate the MODIS BRDF/Albedo product over a heterogeneous agricultural area in the framework of the EODIX campaign. In this way, we applied two BRDF models to AHS airborne data, the RTLSR and the RTLSR-HS, to obtain the surface albedo. The results show good agreement between the RTLSR model (MODIS BRDF/Albedo product algorithm) and the RTLSR-HS model when compared to *in situ* data, with an RMSE of 0.018 in both cases. However, we observed a slight underestimation (more significant in the corn field by the RTLSR model and in the barley field by both models), which has been already reported in previous works such as Roesch, Schaaf, and Gao (2004) and Liu et al. (2009). In fact, we observed that the corn field (in its growth phase in June) and the wheat field (beginning its senescent phase) showed a better agreement with *in situ* data than the barley field (senescent). These facts accord with Jin et al. (2003), who observed good results during the growing season but also observed underestimation during other seasons.
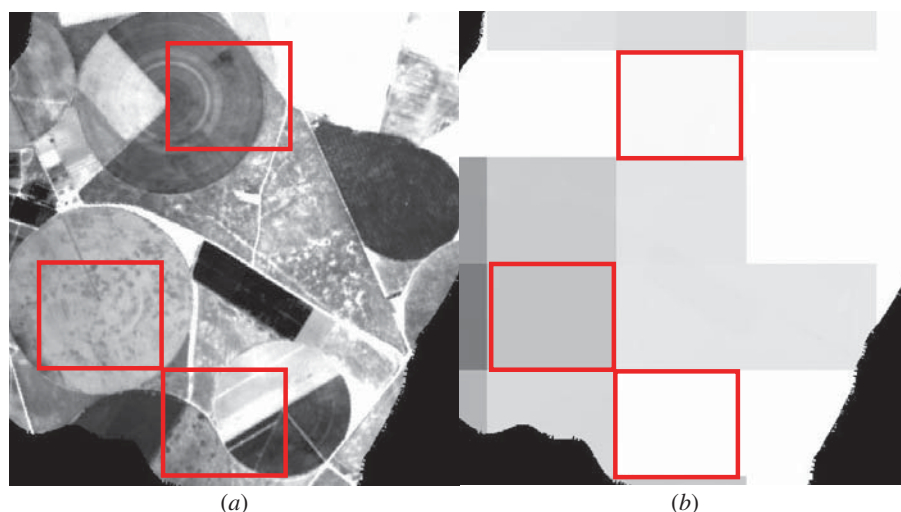

(*a*)   (*b*)

Figure 5.   Blue-sky broadband albedo (*a*) AHS image using the RTLSR model and (*b*) MODIS image. The red *squares over the AHS image* show the equivalent area over MODIS data.
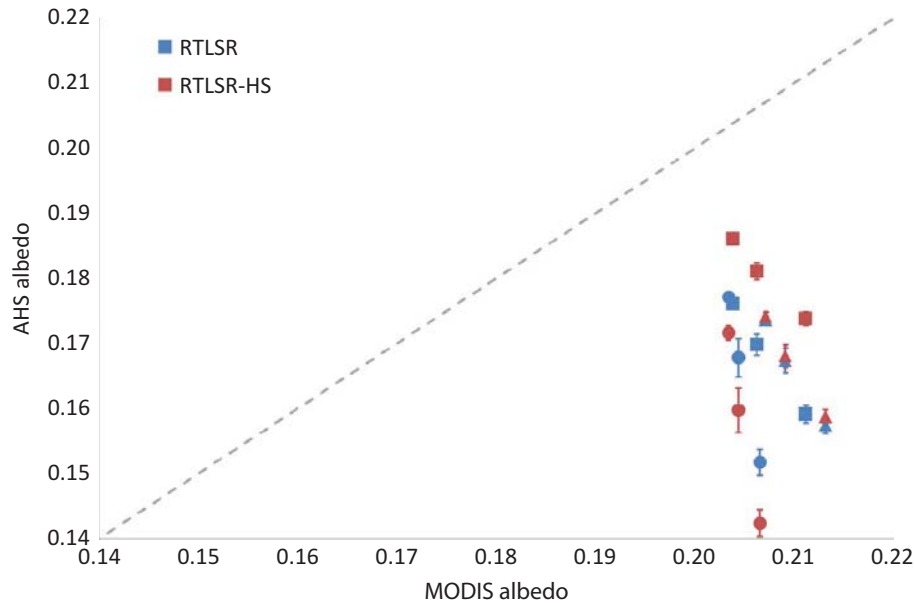
Figure 6.   Comparison between MODIS and AHS albedo for the nearest pixel to the corn (*circles*), wheat (*squares*), and barley (*triangles*) fields.

Regarding the comparison between airborne and satellite data, the aggregation of AHS pixels yielded an RMSE of 0.04 for both models. This error is not simply a consequence of the aggregation technique, but is also due to the methodology applied to estimate BRDF. We must take into account that the MODIS BRDF/albedo algorithm considers that the surface does not change over 16 days, which is a coarse approach when working with agricultural sites near their senescent period. However, the AHS data correspond to a single-day composition. Additionally, we must emphasize the difficulty in comparing satellite to airborne or *in situ* data during this study because of the heterogeneity present. Nevertheless, since airborne images showed good agreement with *in situ* data, the RMSE of 0.04 proves that MODIS BRDF/albedo product meets the required accuracy of 0.02–0.05 in surface albedo estimation. Additionally, in regard to a homogeneous pixel (barley field), we found good agreement between satellite estimation (0.210 ± 0.003) and *in situ* albedo measurement (0.204 ± 0.003).

This article shows that RTLSR and the RTLSR-HS models provide equivalent results. The key difference between both models is in the hot spot region where we did not dispose of *in situ* measurements. Therefore, both models can be used in future studies in albedo estimation, but precision may be slightly enhanced by using RTLSR-HS.

Acknowledgements

References

Barnes, W. L., T. S. Pagano, and V. V. Salomonson. 1998. "Prelaunch Characteristics of the Moderate Resolution Imaging Spectroradiometer (MODIS) on EOS-AM1." *IEEE Transactions on Geoscience and Remote Sensing* 36: 1088–1100.

Cescatti, A., B. Marcolla, S. K. S. Vannan, J. Y. Pan, M. O. Román, X. Yang, P. Ciais, R. B. Cook, B. E. Law, G. Matteucci, M. Migliavacca, E. Moors, A. D. Richardson, G. Seufert, C. B. Schaaf. 2012. "Intercomparison of MODIS Albedo Retrievals and In Situ Measurements Across the Global FLUXNET Network." *Remote Sensing of Environment* 121: 323–334.

Coddington, O., K. S. Schmidt, P. Pilewskie, W. J. Gore, R. W. Bergstrom, M. O. Roman, J. Redemann, P. B. Russell, J. Liu, and C. B. Schaaf. 2008. "Aircraft Measurements of Spectral Surface Albedo and its Consistency with Ground-Based and Space-Borne Observations." *Journal of Geophysical Research*, 113: D17209. doi:10.1029/2008JD010089.

Ferreira, N. C., L. G. Ferreira, A. R. Huete, and M. E. Ferreira. 2007. "An Operational Deforestation Mapping System Using MODIS Data and Spatial Context Analysis." *International Journal of Remote Sensing* 28: 47–62.

Jin, Y., C. B. Schaaf, F. Gao, X. Li, A. H. Strahler, W. Lucht, and S. Liang. 2003. "Consistency of MODIS Surface BRDF/Albedo Retrieval. 1: Algorithm Performance." *Journal of Geophysical Research* 108 (D5): 4158.

Li, X., and A. H. Strahler. 1992. "Geometric-Optical Bidirectional Reflectance Modelling of the Discrete Crown Vegetation Canopy: Effect of Crown Shape and Mutual Shadowing." *IEEE Transactions on Geoscience and Remote Sensing* 30: 276–292.

Liang, S. 2001. "Narrowband to Broadband Conversions of Land Surface Albedo: I. Formulae." *Remote Sensing of Environment* 76: 213–238.

Liang, S., H. Fang, M. Chen, C. Shuey, C. Walthall, C. Doughtry, J. Morisette, C. Schaaf, and A. Strahler. 2002. "Validating MODIS Land Surface Reflectance and Albedo Products: Methods and Preliminary Results." *Remote Sensing of Environment* 83: 149–162.

Liu, J., C. B. Schaaf, A. H. Strahler, Z. Jiao, Y. Shuai, Q. Zhang, M. Roman, A. Augustine, and E. G. Dutton. 2009. "Validation of Moderate Resolution Imaging Spectroradiometer (MODIS) Albedo Retrieval Algorithm: Dependence of Albedo on Solar Zenith Angle." *Journal of Geophysical Research-Atmospheres* 114: D01106.

Lucht, W. 1998. "Expected Retrieval Accuracies of Bidirectional Reflectance and Albedo from EOS-MODIS and MISR Angular Sampling." *Journal of Geophysical Research* 103: 8763–8778.

Maignan, F., F. M. Breon, and R. Lacaze. 2004. "Bidirectional Reflectance of Earth Targets: Evaluation of Analytical Models Using a Large Set of Space-Borne Measurements with Emphasis on Hot-Spot." *Remote Sensing of Environment* 90: 210–220.

Moreno, J., A. Calera, V. Caselles, J. M. Cisneros, J. A. Martínez-Lozano, J. Meliá, F. Montero, and J. A. Sobrino. 2001. "The Measurement Programme at Barrax, in DAISEX Final Results Workshop." *NASA Special Publications* SP-499: 43–51.

Mu, Q., F. A. Heinsch, M. Zhao, and S. W. Running. 2007. "Development of a Global Evapotranspiration Algorithm Based on MODIS and Global Meteorology Data." *Remote Sensing of the Environment* 111: 519–536.

Pu, Z. X., L. Xu, and V. V. Salomonson. 2007. "MODIS/Terra Observed Seasonal Variations of Snow Cover over the Tibetan Plateau". *Geophysical Research Letters* 34: L06.

Roesch, A., C. Schaaf, and F. Gao. 2004. "Use of Moderate-Resolution Imaging Spectroradiometer Bidirectional Reflectance Distribution Function Products to Enhance Simulated Surface Albedos." *Journal of Geophysical Research* 109: D12105. doi:10.1029/2004JD004552.

Roujean, J.-L., M. Leroy, and P. Y. Deschamps. 1992. "A Bidirectional Reflectance Model of the Earth's Surface for the Correction of Remote Sensing Data." *Journal of Geophysical Research* 97: 20455–20468.

Sellers, P. J. 1993. *Remote Sensing of the Land Surface for Studies of Global Change*. Report. Greenbelt, MD: NASA Goddard Space Flight Center.

Sobrino, J. A., J. C. Jiménez-Muñoz, P. J. Zarco-Tejada, G. Sepulcre-Cantó, E. de Miguel, G. Sòria, M. Romaguera, Y. Julien, J. Cuenca, V. Hidalgo, B. Franch, C. Mattar, L. Morales, A. Guillespie, D. Sabol, L. Balick, Z. Su, L. Jia, A. Gieske, W. Timmermans, A. Olioso, F. Nerry, L. Guanter, J. Moreno, and Q. Shen. (2009). "Thermal Remote Sensing from Airborne Hyperspectral Scanner Data in the Framework of the SPARC and SEN2FLEX Projects: An Overview." *Hydrology and Earth System Sciences* 13: 2031–2037.

Strahler A. H., W. Lucht, C. B. Schaaf, T. Tsang, F. Gao, X. Li, J.-P. Muller, P. Lewis, and M. J. Barnsley. 1999. "MODIS BRDF Albedo Product: Algorithm Theoretical Basis Document." NASA EOS-MODIS Doc., V5.0.

Vermote, E. F., D. Tanre, J. L. Deuze, M. Herman, J. J. Morcrette, S. Y. Kotchenova, and T. Miura. 2006. "Second Simulation of the Satellite Signal in the Solar Spectrum (6S)." 6S User Guide Version 3. Accessed November. http://6s.ltdri.org/